Sci. Rep. RITU A39 (1993) pp. 7-14
No. 1, December 1993

Classical MD Simulation and Ab-initio Mixed-basis Band Calculation of C_{60} Adsorbed on Si(100) Surface *

Hiroshi KAMIYAMA[a], Hashem RAFII-TABAR[b], Yutaka MARUYAMA[c], Kaoru OHNO[c] and Yoshiyuki KAWAZOE[c]

[a] *Aomori Public College, 153 - 4 Goushi-Zawa, Yamazaki, Aomori 030, Japan*
[b] *South West London College, Thames Polytechnic, Roehamptom Campus, Manresa House, Holybourne Ave., London SW15, UK*
[c] *Institute for Materials Research, Tohoku University, 2-1-1 Katahira, Aoba-ku, Sendai 980, Japan*

(Received November 30, 1993)

Constant temperature classical molecular dynamics(MD) simulation and *ab-initio* mixed-basis band calculation are carried out to provide a theoretical understanding of for the results of the recent STM experiment concerning the epitaxial growth of C_{60} monolayer film deposited on the Si(100) surface. While performing the classical MD simulation, we often observe c(4 × 3) and c(4 × 4) structures of C_{60} molecules on the Si(100) substrate, and their rotational motions are suppressed by the strong interaction between carbon and silicon atoms. The present theoretical results closely agree with the experimental results of the STM observations of this system. An *ab-initio* band structure calculation using mixed-basis is also performed for the same system. According to this band structure calculation, Fermi surface is concluded to be relatively small around Γ point suggesting electron conduction. The spacial distribution of the partial charge densities calculated for HOMO and LUMO band agrees with the "stripes" observed by STM experiment with negative bias condition.

KEYWORDS: Classical MD simulations, mixed-basis, density functional theory, C_{60}, Si(100) c(2 × 1) surface, Tersoff potential

1. Introduction

It is well known that C_{60} molecule(Buckyball) is a novel form of carbon microclusters having a truncated icosahedron soccer-ball geometry which lies in between smaller carbon clusters and bulk phases. It is also known that this geometry has an unusual degree of stability as a molecule, and in crystalline phase, the C_{60} molecules form the van der Waals molecular solids[1] having an FCC lattice structure with a centre-to-centre distance of 10.2Åwith a rapid rotational motion at room temperature.

Very recently a research throwing a light into the mechanism of epitaxial growth and structural properties of C_{60} molecular thin film deposited on Si(100) c(2 × 1) reconstructed surface has been reported by using field ion STM-based experiment[2]. The Si dimerized surface is "active" since each topmost Si atom forms a dangling bond, and hence it is expected that there would be a significant amount of charge transfer from the dangling bond to the deposited C_{60} molecules. According to the results of the STM experiment, the following conjectures were proposed[2]:
a): The adsorbed C_{60} molecules reside in the troughs of the dimer rows on the surface and are distributed randomly with a minimum separation of 12Å. In this first monolayer film, the individual molecules are surrounded by eight or six dimers of Si surface as depicted schematically in Fig.1.
b): The multilayer deposition of C_{60}'s results in the formation of an FCC crystalline film after the adsorption of the 5th addlayer.
c): There is a short-range ordering of the C_{60}'s in the first monolayer film, and there are two types of molecular alignments, c(4 × 3) and c(4 × 4), emerged on this stable film with the nearest-neighbour distances of 9.6Åand 10.9Å, respectively.
d): STM images often show internal structures of individual C_{60} molecules. In Fig.2 three or four bright rows run in parallel on each molecule. Since the orientations of these "stripes" are the same, this could indicate that the Buckyballs are not rotating on the Si(100) surface even at the room temperature, which is significantly different from the FCC crystalline where the rapid rotational motions(10^9/sec) are observed. The origin of these stripes may be attributed to the transfer of electron charge from the dangling bonds to the molecules.

To obtain a theoretical insight into the dynamics and the interactions of C_{60} molecules with the Si(100) dimerized surface and to examine the validity of the above conclusions, we have performed an *ab-initio* full-potential density-functional calculation and a large-scale classical MD simulation modelling as acculately as possible the experimental procedure for monolayer deposition on the substrate. We have found that our results are in close agreement with most of the above experimental findings.

2. Calculation Methods and Numerical Conditions

2.1. Classical MD simulations

We have applied a classical molecular dynamics simulation to the adsorption of C_{60} molecules onto the Si(100) dimerized surface. The inter-atomic potentials that we have used to describe the Si-Si interactions in the substrate and Si-C interactions between substrate and Buckyballs are Tersoff non-central many-body potentials[3]. These potentials are known to describe well the cohesive energy of covalently-bonded Si and C solids. According to these potentials, the total energy of a system of atoms is modelled as a sum of pairwise interactions with the coefficient of the attractive component, playing the role of a bond order, depending on the lo-

*IMR, Report No. 1947

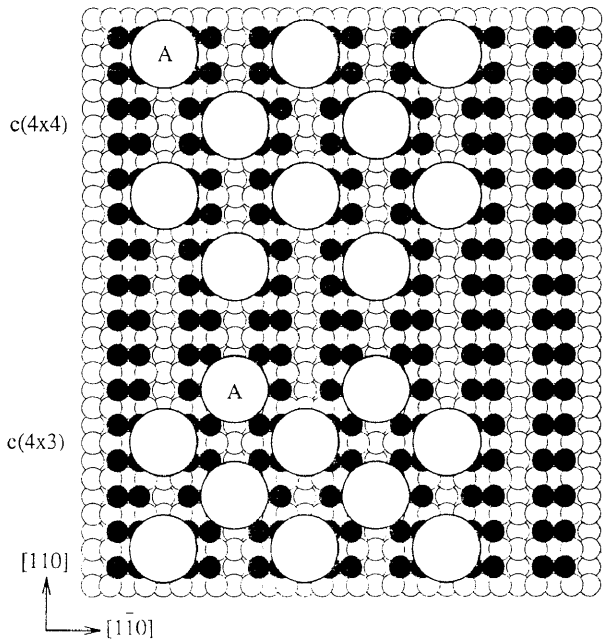

Figure 1. Schematic positions of the C_{60} molecules in the first monolayer film on the Si(100) c(2 × 1) surface showing c(4 × 4) and c(4 × 3) alignments. Open small circles are bulk Si atoms, solid circles are dimerized Si surface atoms, and large open circles are C_{60} molecules. This figure is reproduced from Ref.[2].

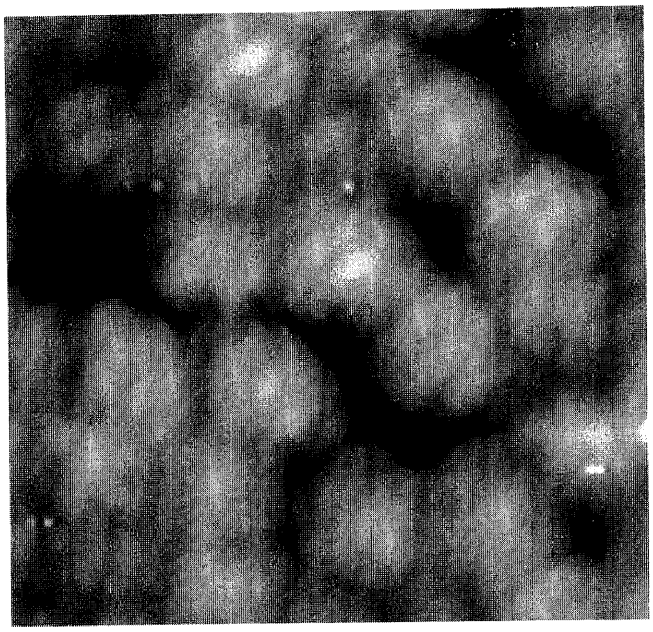

Figure 2. STM image of the first layer of the C_{60} molecules. The image shows some internal structure(three or four rows running in parallel) on individual C_{60} molecule. Figure reproduced from Ref.[2].

cal atomic environment and simulating a many-body interaction. The energy E, as a function of the atomic coordinates, is taken to be:

$$E = \sum_i E_i = \frac{1}{2}\sum_{i\neq j} V_{ij}, \tag{1}$$

$$V_{ij} = f_C(r_{ij})[f_R(r_{ij}) + b_{ij} f_A(r_{ij})], \tag{2}$$

$$f_R(r_{ij}) = A_{ij}\exp(-\lambda_{ij} r_{ij}), \tag{3a}$$

$$f_A(r_{ij}) = -B_{ij}\exp(-\mu_{ij} r_{ij}), \tag{3b}$$

$$f_C(r_{ij}) = \begin{cases} 1, & r_{ij} < R_{ij} \\ \frac{1}{2} + \frac{1}{2}\cos[\frac{\pi(r_{ij}-R_{ij})}{(S_{ij}-R_{ij})}], & R_{ij} < r_{ij} < S_{ij}, \\ 0, & r_{ij} > S_{ij}; \end{cases} \tag{3c}$$

$$b_{ij} = \chi_{ij}(1 + \beta_i^{n_i}\zeta_{ij}^{n_i})^{-1/2(n_i)}, \tag{3d}$$

$$\zeta_{ij} = \sum_{k\neq i,j} f_C(r_{ik})\omega_{ijk} g(\theta_{ijk}), \tag{3e}$$

$$g(\theta_{ijk}) = 1 + c_i^2/d_i^2 - c_i^2/[d_i^2 + (h_i - cos\theta_{ijk})^2]; \tag{3f}$$

$$\lambda_{ij} = (\lambda_i + \lambda_j)/2, \quad \mu_{ij} = (\mu_i + \mu_j)/2, \tag{3g}$$

$$\omega_{ijk} = \exp[\mu_{ik}^3 (r_{ij} - r_{ik})^3], \tag{3h}$$

$$A_{ij} = (A_i A_j)^{1/2}, \quad B_{ij} = (B_i B_j)^{1/2}, \tag{3i}$$

$$R_{ij} = (R_i R_j)^{1/2}, \quad S_{ij} = (S_i S_j)^{1/2}, \tag{3j}$$

where i, j, k label the atoms of the system, r_{ij} is the length of ij bond, and θ_{ijk} is the bond angle between ij and ik. $f_C(r_{ij})$ is a cut-off function and b_{ij} expresses a many-body coupling between the bond from atom i to atom j and the local environment of atom i. Singly subscripted parameters, such as λ_i and n_i, depend only on the type of the atom (C, Si). The parameters in the Tersoff potential are given in Table 1.

The C-C intramolecular interactions inside the C_{60} are described by the harmonic potential:

$$V_{HP}(i,j) = \alpha_{ij}(r_{ij} - r_0)^2 + \beta_{ij}(\omega_{ijk} - \omega_0)^2, \tag{4}$$

where r_{ij} denotes the distance between the atom i and atom j, ω_{ijk} is the bond angle between bond ij and bond ik, and the parameters are taken to be $\alpha_{ij} = 3.5$eV, $\beta_{ij} = 4.0$eV, $r_0 = 1.45$Å, $\omega_0 = 120°$, respectively.

The intermolecular interactions are described with their carbon atoms interacting via Lennard-Jones 12-6 potential:

$$V_{LJ}(i,j) = 4\epsilon[(\frac{\sigma}{r_{ij}})^{12} - (\frac{\sigma}{r_{ij}})^6], \tag{5}$$

Table 1. Parameters of Tersoff potentials for C and Si.

	C	Si
$A(eV)$	1.3936×10^3	1.8308×10^3
$B(eV)$	3.467×10^2	4.7118×10^2
$\lambda(\AA^{-1})$	3.4879	2.4799
$\mu(\AA^{-1})$	2.2119	1.7322
β	1.5724×10^{-7}	1.1000×10^{-6}
n	7.2751×10^{-1}	7.8734×10^{-1}
c	3.8049×10^4	1.0039×10^5
d	4.384×10^0	1.6217×10^1
h	-5.7058×10^{-1}	-5.9825×10^{-1}
$R(\AA)$	1.8	2.7
$S(\AA)$	2.1	3.0
$\chi_{C-C} =$	$\chi_{Si-Si} = 1$,	$\chi_{C-Si} = 0.9776$

where r_{ij} denotes the distance between the atom i and atom j with parameters($\epsilon = 28$K and $\sigma = 3.4\AA$) taken from Ref.[4]. The classical equations of motions are integrated numerically via the velocity Verlet algorithm[5].

The temperature of the system in our simulation is maintained at a fixed value by Nosè algorithm. The energy relaxation during the equilibration stage is performed via a quenched MD algorithm in which the velocities of atoms are quenched to zero at every time steps where the total kinetic energy of the system reached its maximum value.

Basic time step was set to be 2fs and 43,000 steps of the simulation in total, reaching 86ps, is performed in this simulation.

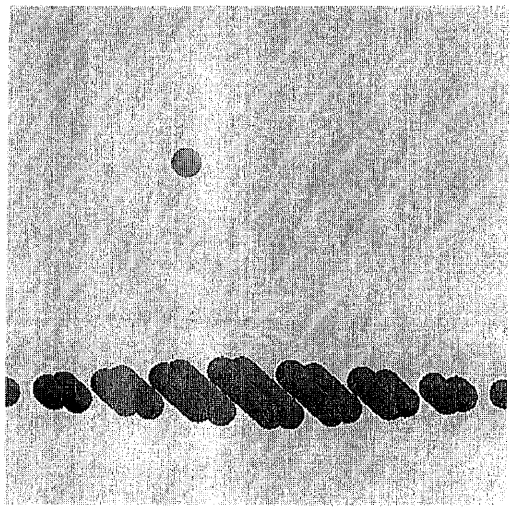

Figure 3. The initial configuration of the one C_{60} molecule separately located above the Si crystal with (100) surface at $t = 0$. Only the center position of C_{60} and the topmost dimer-forming Si atom are drawn in this figure.

The initial configuration consists of one C_{60} molecule settled above the dimerized Si(100) c(2 × 1) substrate in the direction of (001) normal to the surface as shown in Fig. 3. Note that only the center position of C_{60} and topmost dimer-forming Si atoms are drawn schematically in this figure. The substrate consists of 9 atomic layers with 128 Si atoms per layer. With the exception of the Si atoms in the lowermost layer, all other substrate atoms are treated dynamically. The system is equilibrated for 1,000 time steps of Δt=2fs at 300K and at constant pressure. During this stage, the C_{60} is kept sufficiently far from the substrate so that there are no interactions between them.

After equilibration, ten molecules of C_{60} in total are launched in random directions with initial kinetic energy determined randomly corresponding to the room temperature. Since the C_{60} molecules and the surface interact with each other, the molecules move downward, until they reach the surface.

2.2. *Ab-initio* band structure calculation

Band structure calculation is one of the most important methods for investigating the electronic structure of bulk materials. In general, local density approximation in density functional theory together with pseudopotentials and plane wave expansions of wave functions are the presently standard methods to calculate electronic states of materials. Although recent advances in computational power has made it possible to increase the number of basis sets in the expansion of wave functions, resulting in more precise electronic structure calculations, it is rather difficult to deal with light elements such as carbon, boron and nitrogen because the strong Coulomb potential near the nuclei can hardly be removed from the pseudopotentials. Typically 32,000~45,000 plane waves[6] (about 35Ryd to 45Ryd in energy cutoff) are required for simulating the correct bond lengths of small carbon clusters like C_{10} in a pseudopotential formalism. In such a case, the use of pseudopotentials does not reduce the total amount of calculation. Hence for light atoms, the full-potential calculation in dealing with all core electrons as well as all valence electrons is the next desired step towards more precise analysis.

In this paper, we perform an *ab-initio full-potential* band calculation based on the *mixed-basis approach* which uses both Plane Waves(PW's) and the 1s core- and 2p valence-atomic orbitals (AO's). We will apply this method to the C_{60} molecules residing on the Si(100) surface[7, 8].

Historically the mixed-basis approach in the band structure calculation was first introduced by Friedli and Ashcroft[9] in the case of hydrogen molecular crystals, and a similar approach was applied to the case of transition metals by Louie, Ho and Cohen[10] in order to handle the spatial locality and asymmetry of the d-orbitals correctly. The present work is the first attempt to apply the mixed-basis to the two dimensional band structure calculation.

In the mixed-basis formalism, the basis $|l\rangle$ denotes either PW or AO. Suppose that we are using N_{PW} plane waves and $4N_A$ atomic orbitals(1s and $2p_x$, $2p_y$, $2p_z$ orbitals per atom) accompanying the N_A atoms. For $l = 1, \cdots, N_{PW}$ the basis denoting the lth PW is

$$\varphi_l^{PW}(\mathbf{r}) = \langle \mathbf{r}|l\rangle = \frac{1}{\sqrt{\Omega}} e^{-i\mathbf{G}_l\cdot\mathbf{r}}. \qquad (6a)$$

For $l = N_{PW}+1, \cdots, N_{PW}+N_A$ it denotes the 1s atomic wave function (spin is neglected) centered at the $m(=l-N_{PW})$th atom, i.e.

$$\varphi_m^{1s}(\mathbf{r}) = \langle \mathbf{r}|l\rangle = \sqrt{\frac{\alpha_m^3}{\pi}} e^{-\alpha_m|\mathbf{r}-\mathbf{R}_m|}, \qquad (6b)$$

and for $l = N_{PW}+N_A+1, \cdots, N_{PW}+4N_A$ it denotes one of the $2p_x$, $2p_y$, $2p_z$ atomic functions:

$$\varphi_m^{2p_x}(\mathbf{r}) = \langle \mathbf{r}|l\rangle = \sqrt{\frac{\beta_m^5}{\pi}}(x-X_m) e^{-\beta_m|\mathbf{r}-\mathbf{R}_m|}, \qquad (6c)$$

$$\varphi_m^{2p_y}(\mathbf{r}) = \langle \mathbf{r}|l\rangle = \sqrt{\frac{\beta_m^5}{\pi}}(y-Y_m) e^{-\beta_m|\mathbf{r}-\mathbf{R}_m|}, \qquad (6d)$$

$$\varphi_m^{2p_z}(\mathbf{r}) = \langle \mathbf{r}|l\rangle = \sqrt{\frac{\beta_m^5}{\pi}}(z-Z_m) e^{-\beta_m|\mathbf{r}-\mathbf{R}_m|}. \qquad (6e)$$

The effective one-electron Hamiltonian reads

$$H = T + V, \qquad (7a)$$

$$T = -\frac{1}{2}\nabla^2, \qquad (7b)$$

$$V(\mathbf{r}) = -\sum_m \frac{Z_m}{|\mathbf{r}-\mathbf{R}_m|} + \int d\mathbf{r}' \frac{\rho(\mathbf{r}')}{|\mathbf{r}-\mathbf{r}'|} + V^{ec}(\mathbf{r}), \qquad (7c)$$

where we have used the atomic unit (a.u.), $h = m_e = e = 1$. In Eq.(7c), Z_m and $\mathbf{R}_m$ denote, respectively, the atomic number and the position of the mth atom, $\rho(\mathbf{r})$ is the total electron density and $V^{ec}(\mathbf{r})$ the exchange-correlation potential which is evaluated in real space under the local density approximation[11]. In the present formalism, we evaluate $\rho(\mathbf{r})$ directly in real space from the expansion-coefficients determined at the previous step. We also utilize the fast Fourier transform(FFT) for many times in the present algorithm. To calculate the electron-atom and electron-electron Coulomb potentials, i.e the first two terms in Eq.(7c), it is much more efficient to evaluate their sum in the Fourier space as,

$$\bar{V}(\mathbf{G}) = 4\pi \frac{\bar{\rho}(\mathbf{G}) - \sum_m Z_m e^{-i\mathbf{G}\cdot\mathbf{R}_m}/\Omega}{G^2}, \qquad (8)$$

provided that the charge density $\bar{\rho}(\mathbf{G})$ in the Fourier space is known (in Eq.(8) Ω denotes the volume of the unit cell). As a more elaborate matter, in order to perform a high precision integration of potential matrix elements in real space around each atom, meshes on which we evaluate the real space potential are chosen so as to contain the atomic sites at their centers. Therefore we evaluate the real space charge density $\rho_m(\mathbf{r})$ and the potential $V_m(\mathbf{r})$ both centered on the mth atom for $m = 1 \sim N_A$, which is the most time-consuming part in the present computer program.

Once the potential function is determined, we then proceed to evaluate the Hamiltonian matrix elements $\langle l|H|k\rangle = \langle l|T|k\rangle + \langle l|V|k\rangle$. In the calculation of potential matrix elements $\langle l|V|k\rangle$, there are three types of combinations: PW-PW, PW-AO, and AO-AO. For PW-PW the standard calculation in the Fourier space works well. The other combinations PW-AO and AO-AO are more easily calculated in the real space (in the small area around each atomic nucleus), since the 1s and 2p AO's presently chosen are well localized around each of nucleus site. (For such choices of AO's, one may neglect all overlaps between different atomic orbitals located at different nuclei positions as a good approximation.) Moreover, we separate the real-space potential $V_m(\mathbf{r})$ centered on each atom into two parts; one is the spherically-symmetric and analytic part $V_m^a(r) = -6e^{-\zeta_m r}/r$ and the other is the numerical part $V_m^b(\mathbf{r}) = V_m(\mathbf{r}) - V_m^a(r)$. All the relevant integrals involving $V_m^a(r)$ are carried out analytically.

For the matrix elements of the kinetic energy $\langle k|T|k\rangle$, one has three analogous combinations; for PW-PW, PW-1s and PW-2p, i.e.

$$\langle l|T|k\rangle = \frac{1}{2}G_l^2\delta_{lk}, \quad \text{for } 1 \le l,k \le N_{PW}, \qquad (9a)$$

$$\langle l|T|N_{PW}+m\rangle = \frac{4\sqrt{\pi\alpha_m^5}}{\Omega}\frac{G_l^2}{(G_l^2+\alpha_m^2)^2} e^{-i\mathbf{G}_l\cdot\mathbf{R}_m}, \qquad (9b)$$
$$\text{for } 1 \le l \le N_{PW}, \quad 1 \le m \le N_A,$$

$$\langle l|T|N_{PW}+N_A+m\rangle = -i\frac{16\sqrt{\pi\beta_m^7}}{\Omega}\frac{G_l^2 G_x}{(G_l^2+\beta_m^2)^3} e^{-i\mathbf{G}_l\cdot\mathbf{R}_m}, \qquad (9c)$$
$$\text{for } 1 \le l \le N_{PW}, \quad 1 \le m \le N_A,$$

respectively, while, for 1s-1s and 2p-2p, one may expect the hydrogen-like analytic result, $\langle N_{PW}+n|T|N_{PW}+m\rangle = \frac{1}{2}\alpha_n^2\delta_{nm}$ and $\frac{1}{2}\beta_n^2\delta_{nm}$.

Using this *mixed-basis* scheme, a full-potential band calculation is carried out to analyze the two dimensional band structure of the triangular-lattice C_{60} molecules. As the first step to incorporate the effect of the substrate, we model the charge transfer from Si dimers by assuming the charge neutrality with a uniform positive background. There are two distinct sites of C_{60} in the c(4 × 3) structure with six or eight dangling bonds existing nearby. The possible maximum amount of the charge transfer is therefore six per one C_{60}, when we assume that every C_{60} site is geometrically equivalent and all the dangling bonds loose all their electrons. However, less amount of charge transfer seems to be realized in the experiments.

In our calculation, lengths of double and single bonds between two carbons in C_{60} are fixed to be 1.40 and

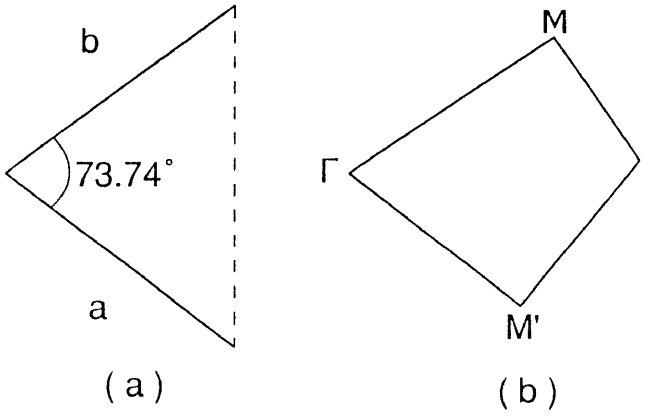

Figure 4. The unit cell and the Brillouin zone. A rhombohedral unit cell having a 73.74° vertex, the lattice constants $a = b = 9.6$Å in the basal plane, and $c = 11.9$Å in the perpendicular direction are used.

1.46Å, respectively, while two double bonds locating on opposite sides of C_{60} are fixed at the lowermost and topmost locations. We assume a rhombohedral unit cell determined experimentally[2] having a 73.74° vertex and $a = b = 9.6$Å(1a.u.=0.52918Å) lattice constants in the basal plane, in which the direction of dimer sequences are parallel to the shorter diagonal of the rhombohedron. With this unit cell, the two distinct C_{60} molecules are approximated to be the same in the c(4 × 3) structure. On the other hand, we use a supercell approximation to treat the vertical direction such that C_{60} repeats in a period of $c = 11.9$Å, which is somewhat larger than a and b. Figure 4 shows the unit cell and the Brillouin zone.

Moreover we take the spin doublet in each level for granted. Sixty 1s atomic orbitals of C_{60} and 1,865 plane waves are adopted as a basis set. The real space is divided into 64 × 64 × 64 meshes, where 3.175 meshes correspond approximately to 0.52918Å. The exponential damping factors $\alpha(=\alpha_m)$ and $\beta(=\beta_m)$ for the 1s and 2p atomic wave functions are chosen as $\alpha = 1/0.101$ and $\beta = 1/0.116$Å^{-1}, respectively.

3. Results and Discussions

3.1. Classical MD simulation

During the equilibration stage, a rotational motion of the C_{60} molecule is initiated from the beginning of this stage. At the end of the equilibration stage, the kinetic energy of the rotational motion reaches the amount corresponding to the room temperature.

Following equilibration, the first C_{60} molecule is launched in a random direction with initial kinetic energy determined randomly corresponding to the room temperature. Since the first C_{60} molecule and the surface interact with each other, the molecule moves downward , until it reaches the surface. After reaching the surface, C_{60} bounces several times giving the kinetic energy to the surface, and finally settle on the surface at

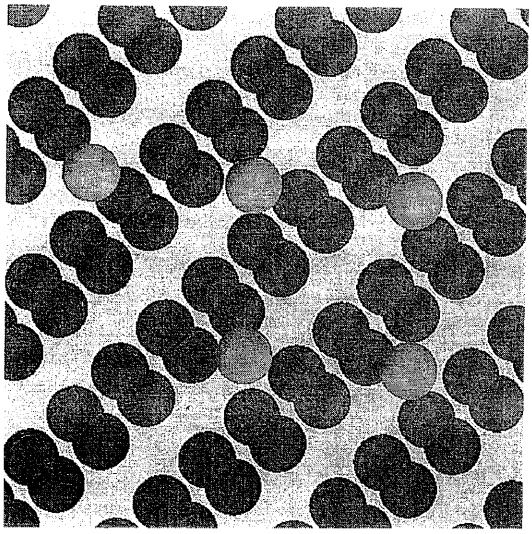

Figure 5. The snapshot of the simulation. Five C_{60}'s form the c(4 × 4) structure at this stage. Sixth C_{60} is approaching from upper-left direction at $t = 42$ps.

the stable point: i.e. it stays at the on-top site of the dimer valley and is surrounded by six dimers as predicted experimentally. At this position, rotational motion of C_{60} is suppressed by the the strong interaction between dimer-forming Si atoms and C atoms of the molecule. This result is in good agreement with conjecture (a) and (d) stated in the Introduction.

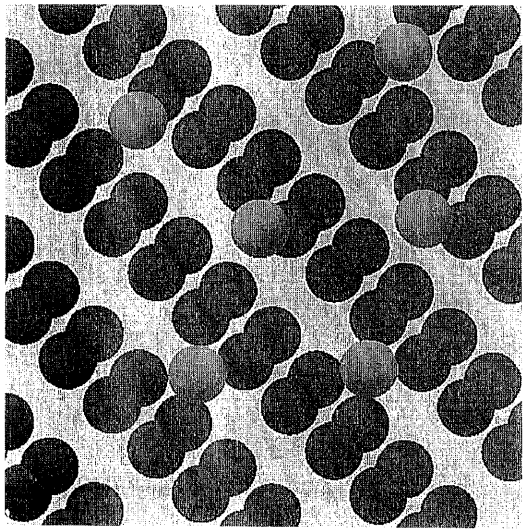

Figure 6. The snapshot of the simulation. The fifth C_{60} hits one of the first layer C_{60} to cause phase transition of c(4 × 4) structure to c(4 × 3) at $t = 49$ps.

After the first C_{60} has settled at stable position, the second C_{60} is launched in a same manner as before. Ten C_{60}'s in total are launched in this simulation. The second molecule goes down interacting with the substrate and with the first C_{60} simultaneously, and is adsorbes onto the surface near the on-top site of the dimer valley next to the first molecule. At this stage, the position of two molecules are slightly distorted because of the intermolecular interaction.

Figure 5 shows a snapshot of the simulation when five C_{60}'s have already been adsorbed on the Si(100) surface and sixth C_{60} is just launched from the top position. It

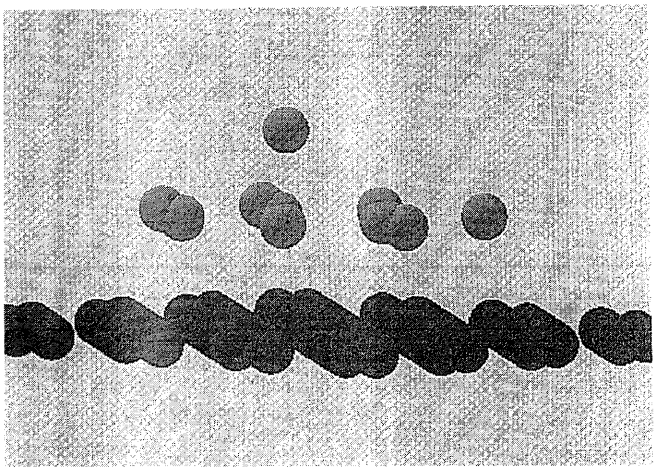

Figure 7. The snapshot of the simulation. The last C_{60} settle onto the first layer to form the close-packed structure at $t = 82$ps.

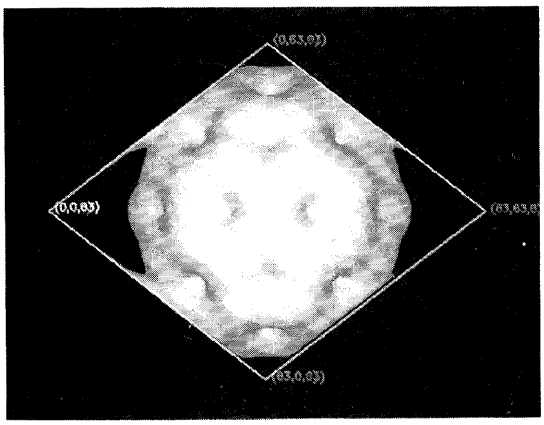

Figure 8. The spatial distribution of total charge density of C_{60} monolayer thin film including 1s core electrons. The charge is localized in the intermolecular region.

is clear that five C_{60}'s form the c(4 × 4) structure which is coherent with the Si(100) dimerized surface, suggesting that c(4 × 4) is one of the most stable structure for this system. It should be noted that the sixth molecule interacts with the substrate and with five C_{60}'s already settled on the surface. Just after this C_{60} reaches the substrate, it repels one of the C_{60}'s on the surface and causes a significant distortion of c(4 × 4) structure to transform to the c(4 × 3) structure(Fig. 6). This result is in agreement with conjecture (c) in Section 1. Furthermore, it should be noted that these structures can be easily distorted by weak perturbations and transform to the other structure.

Figure 7 shows a snapshot when the tenth C_{60} molecule has just settled onto the first monolayer to form the second layer. The position of this molecule is almost the center of a triangle consisted of three molecules at the first layer. A remarkable finding for this molecule is that rotational motions are not suppressed anymore if C_{60} is adsorbed onto the second layer since the strong interaction originated from Tersoff potential does not reach the second layer. While all of the nine molecules at the first layer do not rotate because of the strong interaction between C atom and the dimer-forming Si atom. For all nine molecules, C_2 rotational symmetry axis oriented normal to the surface. The double bonds, vertical to the C_2 symmetry axis, were parallel to the direction of dimer row, for three molecules, while the double bonds of the other six molecules oriented vertical to the dimer row.

We can summarize this part by stating that our large-scale constant temperature classical MD simulation based on the inter-atomic potentials is capable of reproducing most of the experimental results and therefore offer an insight into the dynamics of the Buckyballs on the Si(100) surface.

We now turn to an *ab-initio* band structure calculations that we have carried out for the C_{60} c(4 × 3) thin film structure deposited on Si (100) surface.

3.2. *Ab-initio* band structure calculations

Here, the results of the two-dimensional band structure calculations are presented and compared with the experimental results. Figure 8 shows the spatial distribution of total charge density of C_{60} including 1s core electrons. It is evident that there is a net charge density around the intermolecular region, which has not been observed in the FCC C_{60}[12]. By plotting a contour map near C atom, we have confirmed that there are remarkable concentration of electron charge in the vicinity of C atoms, indicating that 1s core electrons are well described in the present method.

Figure 9 shows the calculated band structure of the C_{60} monolayer thin film. We dropped out from this figure the sixty 1s bands all locating at -22Ryd. without dispersion, while we depicted the first 30 valence levels. Because of the existence of strong dispersion, there are band overlaps everywhere, and the overall feature is quite different from that obtained for the FCC C_{60}[12], although the density of state is rather similar. This feature originates from both the existence of two-dimensional crystal field, and the decrease of nearest-neighbor distance between molecules (about 1Å smaller than that for the FCC). When there is some amount of charge transfer from Si substrate, the lower 121 levels are completely occupied and the 122nd and 123rd levels are partly occupied, where the Fermi level exists (denoted E=0 in Fig.9) It should be noted that HOMO band in the present calculation is not degenerate at Γ point, which is quite different from that in FCC C_{60}.[12] The band structure of C_{60}^{4-} and C_{60}^{6-} are also calculated and similar results are obtained. From Fig.8 we see that the Fermi surface around Γ point is very small, indicating the existence of small number of surface free carriers.

Figure 10 shows the spatial distribution of the partial charge density of the HOMO band at the Γ point. This band is made of top three levels below the band gap. On the other hand, Fig. 11 shows the spatial distribution of the partial charge density of the lowest level belonging to the LUMO band at the Γ point. It is easily seen that

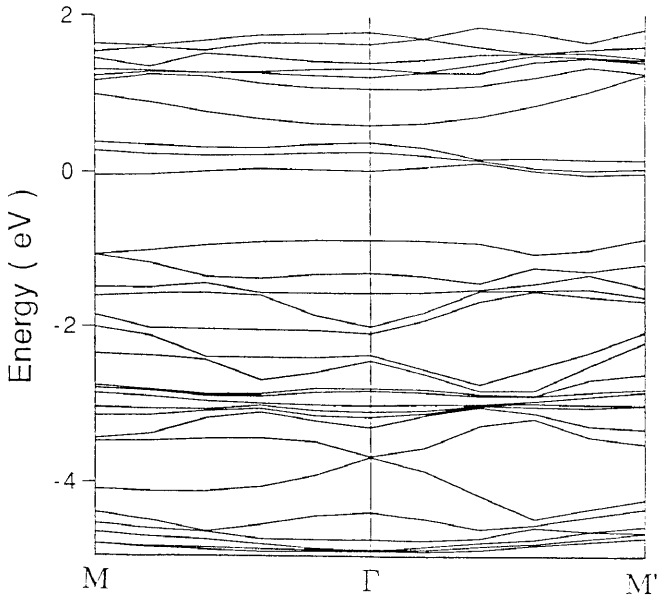

Figure 9. The calculated band structure of the C_{60} monolayer thin film. Sixty 1s bands are dropped out from the figure.

there is a set of "stripes" in the isosurface of Figs. 10 and 11 parallel to the direction of the topmost double bond of C_{60}. This feature corresponds to the STM image[2] in good agreement with the conjecture (d) mentioned before, and suggests the agreement between the theory and experiment. We have confirmed that the direction of stripes always coincides with the direction of topmost double bond. This result suggests that one can determine the orientation of C_{60} from the STM pattern image by identifying the direction of stripes.

We can summarize this part by stating that *ab-initio* all-electron calculations using the *mixed-basis* can reproduce the density of states and the 1s binding energy for the carbon system correctly. The results of our band structure calculations explain accurately the experimental findings concerning the charge transfer from silicon substrate to the C_{60}, and give a theoretical insight into the nature of the "stripes" observed on the C_{60} molecules. We ascertain that these "stripes" must arise as a result of the charge transfer.

4. Concluding Remarks

We have performed a Classical Molecular Dynamics simulation and an *ab-initio full-potential* band structure calculation simultaneously, and applied them to C_{60} monolayer thin film adsorbed on the Si(100) dimerlized surface. We have found that our results are in close agreement with the experimental findings. All the results are summarized in the last part of Sections 3.1 and 3.2, for the Classical MD and *ab-initio* studies, respectively. These two approaches and results are mutually complementary, and simultaneous studies enable us to

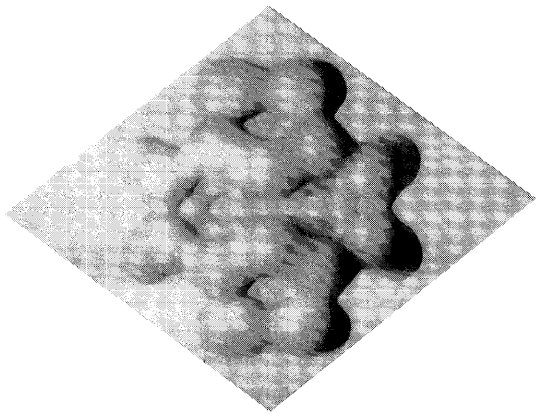

Figure 10. The spatial distribution of the partial charge density of the HOMO band at the Γ point.

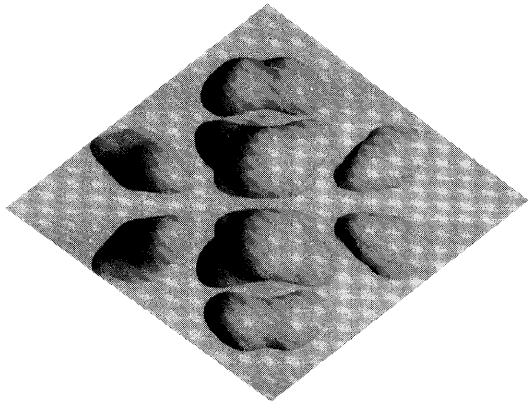

Figure 11. The spatial distribution of the partial charge density of the lowest level belonging to the LUMO band at the Γ point.

give a theoretical insight into the dynamics and the mechanics(details of the interactions) of this system.

Acknowledgements:

The authors are grateful to Professors Y. Nishina, T. Sakurai and T. Hashizume at our Institute for introducing us to their new STM-based experimental results, and to Professor K. Shindo for a lot of valuable discussions in proceeding our *ab-initio* calculation. They also thank the members of the Computer Science Group at the Institute for Materials Research. They are also indebted to IBM Japan, Kubota Computer Inc., and Japan IMSL Inc. for providing extensive computational facilities.

1) C.S. Yannoni, R.D. Johnson, G. Meijer, D.S. Bethune, and J.R. Salem, "^{13}C NMR study of the C_{60} cluster in the solid states: Molecular motion and carbon chemical shift anisotropy", *J. Phys. Chem.*, **95**, 9 (1991).

2) T. Hashizume, X.-D. Wang, Y. Nishina, H. Shinohara, Y. Saito, Y. Kuk, and T. Sakurai, " Field ion-Scanning Tunnelling Microscopy study of C_{60} on the Si(100) surface", *Jpn.J.Appl. Phys.*, **31**, L880 (1992).

3) J. Tersoff, "Modelling solid-state chemistry: Interatomic potentials for multicomponent systems", *Phys. Rev.*, **B39**, 5566 (1989).

4) A. Cheng and M. Klein, " Molecular-dynamics investigation of orientational freezing in solid C_{60}", *Phys. Rev.*, **B45**, 1889(1992).

5) M.P. Allen and D.J. Tildesley, *Computer Simulation of Liquids*, Clarendon Press, Oxford, (1987).

6) W. Andreoni, D. Scharf and P. Giannozzi, "Low-temperature structures of C_4 and C_{10} from the Car-Parrinello method: singlet states", *Chem. Phys. Lett.*, **173**, 449 (1990).

7) H. Kamiyama, K. Ohno, Y. Maruyama, and Y. Kawazoe, "*Ab-initio* molecular dynamics simulation of C_{60}", *Proc. Int. Symp. on the Physics and Chemsitry of Finite Systems*, edited by P. Jena et al, Kluwer Academic Publishers, **Vol. II**, 1335 (1992).

8) H. Kamiyama, K. Ohno, Y. Maruyama, Y. Kawazoe, Y. Nishina, "Ab-initio Molecular Dynamics Simulation of Monolayer C_{60} Thin Film on Silicon (100) Surface", *Z. Phys. D*, **26**, 5291(1993).

9) C. Friedli and N. W. Ashcroft, "Combined representation method for use in band-structure calculation: Applicaton to highly compressed hydrogen", *Phys. Rev.*, **B16**, 662 (1977).

10) S. G. Louie, K.-M. Ho and M. L. Cohen, "Self-consistent mixed-basis approach to the electronic structure of solids", *Phys. Rev.*, **B19**, 1774 (1979).

11) W. Kohn and L. J. Sham, "Self-consistent equations including exchange and correlation effects", *Phys. Rev.*, **140**, A1133 (1965) & L. Hedin and B. I. Lundqvist, "Explicit local exchange correlation potential", *J. Phys.*, **C4**, 2064 (1991).

12) S. Saito and A. Oshiyama, " Cohesive mechanism and energy bands of solid C_{60}", *Phys. Rev. Lett.*, **66**, 2637(1991); B.-L. Gu, Y. Maruyama, J.-Z. Yu, K. Ohno, and Y. Kawazoe, "Effects of Molecular Orientation on the Electronic Structure of fcc C_{60}", Phys. Rev. **B**, to be published.